Al^{18}F-AEEA-HER2-BCH Affibody Reveals Clearer PET Imaging Than ^{18}F-FDG in Patients With Breast Cancer: A Pilot Clinical Translation Study

Xiaoyi Guo
beijing cancer hospital
Nina Zhou
Beijing cancer hospital
Jin Ding
Beijing Cancer Hospital
Shuailiang Wang
Beijing Cancer Hospital
Teli Liu
Beijing Cancer Hospital
Guohong Song
Beijing Cancer Hospital
Hua zhu
Beijing Cancer Hospital
Zhi Yang (pekyz@163.com)
Peking University Cancer Hospital & Institute https://orcid.org/0000-0003-2084-5193

Research Article

Keywords: Al18F-HER2-BCH, Breast Cancer, Human Epidermal Growth Factor Receptor 2, 18F-FDG, PET/CT

Posted Date: October 21st, 2021

DOI: https://doi.org/10.21203/rs.3.rs-993783/v1

Abstract

Purpose To construct, validate and preclinically evaluate a novel HER2 target agent Al^{18}F-AEEA-HER2-BCH affibody (Al^{18}F-HER2-BCH), and perform a pilot clinical translational study in HER2-positive breast cancer patients.

Methods In preclinical study, the HER2 target specificity were verified using HER2-positive and HER2-negative cells and mice models. In clinical study, we enrolled 14 HER2-positive breast cancer patients (7 newly diagnosed patients and 7 relapsing metastatic patients) and one HER2-negative breast cancer patients. The safety were observed and lesion detection ability was compared with ^{18}F-FDG in 14 HER2-positive breast cancer patients (NCT04547309). All patients injected with 222±18.5 MBq Al^{18}F-HER2-BCH and scanned at 2 h and 4 h, and received standard ^{18}F-FDG PET/CT scan within 7 d.

Results In preclinical study, the Kd value of Al^{18}F-HER2-BCH was 25.5±2.53 nM. Micro-PET imaging of Al^{18}F-HER2-BCH showed significantly higher tumor uptake in HER2-positive NCI-N87 models than in HER2-negative MDA-MB-231 models (12.2±1.08 ID%/g vs 1.25 ± 0.25 ID%/g, $p < 0.0001$). In clinical study, for the 7 newly diagnosed breast cancer patients, Al^{18}F-HER2-BCH depicted more primary lesions than ^{18}F-FDG (9 vs 6), with higher tumor/breast (T/B) ratio (17.9±13.2 vs 5.4±3.4, p<0.05). And Al^{18}F-HER2-BCH detected more metastatic lymph nodes than ^{18}F-FDG (20 vs 7) with higher uptake (SUVmax, 6.42±3.84 vs 5.1±1.06). For the 7 relapsed metastatic patients, Al^{18}F-HER2-BCH presented better metastases detection ability than ^{18}F-FDG (93 vs 45), especially lymph node (39 vs 23), bone (39 vs 21), and liver metastases (30 vs 3). Compared with ^{18}F-FDG, Al^{18}F-HER2-BCH upstaged 5/7 newly diagnosed breast cancer patients and detected more distant metastases in 4/7 relapsed patients.

Conclusions The findings described here demonstrated that Al^{18}F-HER2-BCH had high affinity and target specificity, and it was feasible to detect HER2-positive lesions in primary and metastatic breast cancer patients.

Introduction

As of 2020, female breast cancer has now surpassed lung cancer as the leading cancer in terms of global incidence, with an estimated 2.3 million new cases, accounting for 11.7% of all cancer-related deaths. It is the fifth leading cause of cancer-related mortality worldwide, with a 5-year survival rate of 31.4%[1 2]. HER2 is a transmembrane receptor of the tyrosine kinase family, which overexpress in approximately 15-20% of newly diagnosed breast cancer patients and regulate cell growth, survival, differentiation, angiogenesis and DNA repair[3 4]. Trastuzumab, an anti-HER2 monoclonal antibody, was approved for the treatment of advanced breast cancer by the Food and Drug Administration (FDA) in 1998. Several evidences have demonstrated that trastuzumab therapy is associated with a complete pathological response to 23-26% in patients with HER2 positive advanced breast cancer, while when adding chemotherapy to the trastuzumab therapy protocol, better results were reported[5]. However, HER2-targeted therapy fails in 50-

70% of patients with HER2-positive breast cancer even with combination treatments[6 7]. The widely resistance of the biological mechanisms are not completely understood. Therefore, identifying and characterizing in situ biomarkers of HER2 status can help to overcome trastuzumab resistance.

The HER2 expression in tumors is highly heterogeneous and it may change during the treatment. Pathological examination is an invasive examination, which is not suitable for repeated operation and it is difficult to solve the problem of heterogeneity. The HER2 status is hard to evaluated according to MRI/CT-detected signal intensity[8 9]. ^{18}F-Fludeoxyglucose (FDG) PET/CT is a valuable imaging modality in the management of patients with breast cancer in stage IIIA or higher[10–16]. However, the sensitivity of ^{18}F-FDG for brain and liver lesions is low[17]. The accurate, dynamic and noninvasive detection of HER2 status during treatment remains a challenge.

Several studies have utilized radiolabeled intact HER2 antibody for targeting HER2 in the preclinical or clinical setting in breast cancer[18–21]. As reported, ^{64}Cu (T1/2 = 12.7 h) and ^{89}Zr (T1/2 = 78.4 h) used to label HER2 antibody, such as trastuzumab and pettuzumab, for the clinical PET imaging of HER2 in patients with gastric cancer and breast cancer. HER2 affibody ZHER2:342 (ABY-002, ABY-025) was labeled with ^{68}Ga, evaluated for molecular imaging in breast cancer patients.

Fluorine-18 is an ideal PET imaging agent due to its optimal half-life of 110 min. It has been widely used to develop various tracers to image receptors and assess uptake and pathway status in the body[22]. Moreover, automated methods of radiolabeling have been developed using Current Good Manufacturing Practice (cGMP) guidelines for clinical use to promote clinical application. We added aminoethy lethanolamine (AEEA) and 6-aminocaproic acid (ACP-6) aminocaproic acid at the amino and carboxyl sides of the ZHER2:342 affibody structure to construct AEEA-HER2-affibody-BCH. In this study, we used the Al^{18}F-AEEA-HER2-affibody-BCH (hence abbreviated as Al^{18}F-HER2-BCH) reagent to assess its safety, feasibility, biodistribution, and tumor targeting ability in HER2-positive breast cancer patients.

Materials And Methods

Al^{18}F-HER2-BCH Preparation and Quality Control

NOTA-HER2-affibody-BCH was synthesized using a solid-phase strategy conducted by the China Peptides Company. The radiosynthesis of Al^{18}F-HER2-BCH was as follows: premixed 100 μl ^{18}F (0.37-3.7 GBq), 11 μl potassium hydrogen phthalate (KHP) (0.5 M, pH 4.0), 6 μl AlCl3 (2 mM), and 100 μl ethyl alcohol at room temperature for 5 min. Then, added 500 ug HER2-affibody-BCH (50 μl, 10 mg/ml), mixed well, and reacted at 100 ℃ for 15 min[18]. The details of the radiolabeling, quality control conditions and stability were described in the supplemental materials.

Preclinical Study

Cell study HER2 (+) NCI-N87 and HER2 (-) MDA-MB-231 cell lines were chosen for *in vitro* cell uptake study. 0.5 mL of 74 KBq Al^{18}F-HER2-BCH in fresh medium was added into each well and incubating for 10 min, 30 min, 1 h, 2 h, 3 h and 4 h. For the blocking experiment, cells were co-incubated with 50 μg HER2-affibody-BCH per well. The Kd of Al^{18}F-HER2-BCH was determined by adding different concentrations of radiotracer to N87 cells. The details could be seen in supplemental materials.

Micro-PET study 4.8 MBq of Al^{18}F-HER2-BCH was injected into each of BALB/c female mice bearing NCI-N87 and MDA-MB-231 tumors with or without 200 μg HER2-affibody-BCH *via* the tail vein. The mice were anesthetized with 3% (v/v) isoflurane and underwent a Super Nova PET/CT scanner (PINGSENG Healthcare (Kunshan) Inc.) with continuous 1% (v/v) isoflurane. Micro-PET scans were conducted at 1, 2, and 4 h after injection. The counts of regions of interest (ROI) over tumor, kidney and muscle were collected.

Bio-distribution Mice bearing NCI-N87 and MDA-MB-231 tumors were injected with 0.74 MBq of Al^{18}F-HER2-BCH (0.2 ml) with or without 200 μg HER2-affibody-BCH *via* the tail vein. The mice were sacrificed in groups (n = 4) at 0.5, 1, 2, and 4 h postinjection. The heart, liver, lung, kidney, spleen, stomach, bone, muscle, blood, other gastrointestinal organs and tumors were collected and weighed, and the radioactivity was measured with a γ-counter.10 samples of 1.0% injected dose were measured at the same time intervals as a standard. The results were expressed as the percent of injected dose per gram (%ID/g).

Radiotoxicity Al^{18}F-HER2-BCH was injected at a dose of 1.55 GBq/kg to each of KM female mice (200 μL, n=7, 20.7 ± 2.2 g, 5 weeks). In the control, 7 mice were injected with 200 μL of saline. The weight and routine orbit blood were monitored for 7 d, and liver function and renal function were detected on the 7th (see supplemental materials for details).

Clinical Study

Patient Enrollment This study was a single-center clinical trial, approved by the Medical Ethics Committee of Peking University Cancer Hospital and American Center for Clinical Trial Management (Ethics Approval License No.2019KT114 and NCT04547309). The patients included in this study had pathologically confirmed HER2-positive (IHC 3+ or IHC 2+/FISH+) breast cancer. Inclusion criteria were as follows: congestive heart failure, severe liver or kidney dysfunction, pregnant or lactating. Ongoing treatment was not an exclusion criterion. All patients provided written informed consent before participating in the study.

Al^{18}F-HER2-BCH and ^{18}F-FDG PET/CT imaging

Each patient was injected with 222±18.5 MBq of Al^{18}F-HER2-BCH and 500 μg HER2-affibody-BCH as our previous study[23] to reduce the non-specific uptake of liver. For the first patient, serial whole-body dynamic PET acquisitions were performed immediately after injection (0-40 min dynamic scan, 6 passes) and a static whole-body scan at 2 h and 4 h. The other 13 patients were scanned at 2 h and 4 h. All patients underwent ^{18}F-FDG (3.7 MBq/Kg) PET/CT scan at 1 h post injection within 7 d, with fasting at least 6 h before imaging.

Imaging was performed on a Biograph mCT Flow 64 scanner (Siemens, Erlangen, Germany), ranging from the apex of the skull to the mid-thigh. The axial field of view of PET was 21.6 cm. PET was acquired in 3-dimensional mode flow motion (bed entry speed 1 mm/s). Reconstruction was performed on Siemens Company Multimodality Workplace (MMWP) by the TrueX+TOF method; attenuation correction was performed using the unenhanced low-dose CT data.

Image Analysis

The imaging were interpreted by two experienced radiologists. Quantification of Al^{18}F-HER2-BCH uptake was performed using a volume of interest (VOI) analysis method, and the mean standard uptake (SUVmean) values and the maximum standard uptake (SUVmax) were calculated. A positive PET lesion was defined as an SUVmax greater than that of the baseline mediastinal blood pool.

Statistics

The Kd value were calculated by One site-Specific binding respectively with GraphPad Prism 5.0[18]. Differences between uptake (% IA/10^6 cells, %ID/g, SUVmax) of two tracers were assessed using the wilcoxon signed-rank test included in GraphPad Prism 5.0. Differences with a P-value less than 0.05 were considered statistically significant.

Results

Preparation and Preclinical Evaluation of Al^{18}F-HER2-BCH

Al^{18}F-HER2-BCH was prepared with a nondecayed corrected radiochemical yield of 45.2% ± 10.5% (n=20). The radiochemical purity reached 98.2% ± 0.2% with a specific activity of 15.6-24.2 GBq/μmol (n>20). The results of quality control were shown in **Figure S1**. Radio-HPLC analysis of the radiotracers revealed no aggregates, fragments, or radioactive purities. In vitro stability, Al^{18}F-HER2-BCH was stable in both saline and 5% HSA within 6 h. In vivo stability, after the mice were injected with the radiotracer for 30 min, the radio-HPLC results of blood showed the main peak (>90%) at retention time of 10.26 min, which was close to that of Al^{18}F-HER2-BCH (T=9.85), indicating that Al^{18}F-HER2-BCH was stable without significant decomposition in 30 min.

Cell uptake and Kd study

As shown in Figure 1A, Al^{18}F-HER2-BCH showed significantly higher uptake in NCI-N87 cells than in MDA-MB-231 cells (1.95±0.24% vs 0.54±0.02 % IA/10^6 cells, p< 0.0001, 2 h) within 4 h. The uptake of Al^{18}F-HER2-BCH in NCI-N87 cells decreased sharply when co-injection of 50 μg HER-affibody-BCH (0.41±0.13 %IA/10^6 cells, p< 0.0001, 2 h), indicating that Al^{18}F-HER2-BCH had good specificity. The Kd value of Al^{18}F-HER2-BCH to HER2 in NCI-N87 cells was determined to be 25.53±2.29 nM (Figure 1B).

Bio-distribution study The uptake of Al^{18}F-HER2-BCH in the NCI-N87 tumors was obviously higher than in MDA-MB-231 tumors (12.2±1.08% ID/g vs 1.46 ± 0.57 %ID/g, $p < 0.0001$) at 2 h, and the tumor uptake was blocked to 1.46 ± 0.57 %ID/g by coinjection of 500 μg HER-affibody-BCH **(**Figure 1D**)**.

Micro-PET imaging study As showed in Figure 1E, Al^{18}F-HER2-BCH depicted clearly tumor uptake at 1 h, maintain high uptake until 4 h. Compared with MDA-MB-231 models, Al^{18}F-HER2-BCH showed significantly higher uptake in the NCI-N87 models during whole imaging. When 500 μg HER2-affibody-BCH was coinjected, the uptake in the N87 models markedly decreased further confirmed the specific uptake. The tumor-to-muscle (T/M) ratios of NCI-N87 was higher than MDA-MB-231 and NCI-N87 block, with T/M values of 8.03, 1.27, 1.41 at 2 h, respectively **(**Figure 1C**)**.

Pathological examination Figure 1F described the HE staining and IHC results of NCI-N87 tumors and MDA-MB-231 tumors. IHC results showed high expression in NCI-N87 tumors and low expression in MDA-MB-231 tumors, which consistent with the results of bio-distribution and micro-PET imaging of Al^{18}F-HER2-BCH.

Radiotoxicity

No significant differences in weight, hematologic markers, liver function tests or renal function tests were observed between the mice injected with Al^{18}F-HER2-BCH (1.48 GBq/kg) and those injected with saline within 1 week of growing ($p>0.05$, **Figure S2 and Figure S3**). In addition, no lethal or chronic toxicity, hematologic effects, or biochemical effects were observed.

Clinical study in BC Patients

Patient characteristics Between June 2020 and February 2021, 14 HER2-positive breast cancer patients and one HER2-negative breast cancer patient were completed the study protocol. Among them, 7 patients were newly diagnosed and had not received any treatment. Totally 9 primary lesions in 7 newly diagnosed patients were pathologically confirmed. The other 7 patients relapsed during follow-up according to increased tumor markers or other features on imaging examinations.

The optimal time point for Al^{18}F-HER2-BCH PET/CT imaging

Dynamic imaging showed blood pool activity was initially high, decreased rapidly in the first 8 min, and was then followed by a slower decrease until 32 min. High uptake was noticeable in both the liver and spleen in the first 8 min. Uptake in the glands (lacrimal gland, parotid gland, submandibular gland and thyroid gland) and other tissues increased gradually. The tumor could be visualized at 8 min, exceeded the blood pool activity after 30 min, and maintained high accumulation throughout the examination. Static images were collected for 2 h and 4 h. The high uptake of Al^{18}F-HER2-BCH was observed in the glands, liver, kidney, and tumor at 2 h, and slightly changed at 4 h **(**Figure 2 **and Figure S4)**.

^{18}F-FDG and Al^{18}F-HER2-BCH PET/CT imaging in newly diagnosed patients

Al^{18}F-HER2-BCH detected more primary lesions than ^{18}F-FDG (9/9 vs 6/9). The background of normal breast tissue on ^{18}F-FDG and Al^{18}F-HER2-BCH were both low (1.02±0.4 and 0.6±0.2). Al^{18}F-HER2-BCH showed a higher tumor-to-background contrast and clearer tumor delineation than ^{18}F-FDG, with tumor/breast (T/B) ratios of 17.9±13.2 vs 5.4±3.4 (p<0.05) **(**Table 1**)**. The primary breast cancer included 5 nodular lesions and 4 non-nodular lesions. ^{18}F-FDG uptake in the nodular lesions was higher than non-nodular lesions(9.7±0.60 vs 2.9±0.36, *p<0.0001*), while Al^{18}F-HER2-BCH uptake showed no difference between two groups (12.23±6.67 vs 8.63±0.49, *p=0.165*). (Figure 3**).** In addition, as showed in **Figure S5**, Al^{18}F-HER2-BCH could also detect the other HER2-positive small lesion of the patient, which was HER2 3+.

For metastatic lymph nodes detection, Al^{18}F-HER2-BCH detected more lesions than ^{18}F-FDG (20 vs 7), and the uptake was higher (SUVmax, 6.42±3.84 vs 5.1±1.06). The average diameter of lymph nodes detected by Al^{18}F-HER2-BCH was 0.72 cm, and the smallest one was only 0.29 cm. As depicted in Figure 4, Al^{18}F-HER2-BCH more clearly showed the primary tumor and the involved axillary lymph nodes than ^{18}F-FDG in a HER2-positive primary diffuse breast cancer patient. Puncture pathology showed that the primary focus was HER2 3+, proving that the patient was a HER2-positive patient.

Both images revealed no distant metastasis in the 7 patients.

Moreover, Al^{18}F-HER2-BCH changed TNM stages classified by ^{18}F-FDG. One patient changed from T0 to T1, one patient changed from T2 to T3, two patients changed from N1 to N2, and one patient changed from N1 to N3.

Diagnostic performance of ^{18}F-FDG and Al^{18}F-HER2-BCH PET/CT in relapsed patients

Al^{18}F-HER2-BCH detected visceral metastases in 7 of 7 patients (100%), while ^{18}F-FDG detected them in 5 of 7 patients (71.4%), missed 1 patients with liver and bone metastases and 1 patient with liver metastases. In addition, Al^{18}F-HER2-BCH detected more bone metastases in 2/5 patients **(**Figure 5**)**. Among 7 patients, 93 lesions (19 lymph node metastases, 39 bone metastases, 30 liver metastases, and 5 lung metastases) were selected for analyses of two images. The number of lesions and the semi-quantitative parameters were presented in Table 2 **and Figure S6**.

Al^{18}F-HER2-BCH detected more positive lymph nodes (19 vs 14), with higher uptake than ^{18}F-FDG (9.54±7.75 vs 5.78±1.86). The diameter of lymph nodes ranged from 0.42 cm-3.88 cm, with an average value of 1.01 cm. For bone metastasis, Al^{18}F-HER2-BCH detected more lesions (39 vs 21), with higher uptake than ^{18}F-FDG (13.57±6.90 vs 4.62±3.68, p<0.0001).Al^{18}F-HER2-BCH also detected more liver metastases (30 vs 3), with higher uptake than ^{18}F-FDG (8.7±4.17 vs 3.2±0.61). The smallest liver metastatic lesion was only 0.61 cm, For lung metastases, the uptake of ^{18}F-FDG was higher than that of

Al^{18}F-HER2-BCH (5.50±2.25 vs 4.26±1.89, *p*=0.41), and lesions detected by two images was same (5 vs 5) (Table 2).

Diagnostic performance of ^{18}F-FDG and Al^{18}F-HER2-BCH PET/CT in HER2-negative patient

As described in **Figure 6**, ^{18}F-FDG showed high uptake in the bone metastases in a HER2-negative breast cancer patient with recurrence, while there was relatively low uptake in the same lesion sites of Al^{18}F-HER2-BCH. The pathological results of the breast lesions showed HER2 2+, and FISH test showed no amplification, proving that the patient was a HER2-negative patient. The HE staining results could be seen in **Figure S7**.

Discussion

Molecular imaging is a whole-body, noninvasive and dynamic medical imaging technology, that provides detailed images of what is happening at both the cellular and molecular levels inside the human body. HER2 status is an important tumor characteristic for guiding treatment in patients with breast cancer. We have successfully developed HER2-targeted antibody molecular probes, ^{64}Cu-NOTA-trastuzumab[24] and ^{124}I-trastuzumab[25], as PET/CT imaging agents in the clinical imaging of patients with gastric cancer. Due to the slow clearance of radioactivity from antibodies in the blood and normal organs, we explored a small-scaffold HER2 radiotracer (^{68}Ga-NOTA-MAL-MZHER2) and evaluated the sensitivity, specificity and utility for HER2-targeted imaging in patients with advanced gastric cancer (AGC)[23 26],and it was feasible to noninvasively detect the HER2 status in AGC patients and enable early detection with a low dose.

To increase the efficiency of ^{18}F labeling and improve the stability in vivo, we successfully constructed a novel Al^{18}F-HER2-BCH that could be efficiently radiosynthesized in an easier process with a favorable nondecayed radiochemical yield (45.2±10.5%) within 30 min. Regarding the overall results of the different imaging modalities among the 14 patients initially assessed, Al^{18}F-HER2-BCH upstaged 5/7 patients with newly diagnosed breast cancer and detected more visceral metastases than ^{18}F-FDG in 4/7 (57.1%) patients with relapsed breast cancer. Combined with the pathological results of the primary lesions, it was verified that there was high uptake of Al^{18}F-HER2-BCH in the tumor sites with high HER2 expression. In addition, Al^{18}F-HER2-BCH showed relatively low tumor uptake in a HER2-negative patient who with HER2 2+ and FISH-, further confirmed the HER2 target specificity.

For the detection of primary focus of newly diagnosed breast cancer patients, Al^{18}F-HER2-BCH showed a clearer tumor delineation and a higher tumor-to-background contrast than ^{18}F-FDG. For the detection of lymph node metastases, Al^{18}F-HER2-BCH showed better detection capability than ^{18}F-FDG (39 vs 21). Moreover, more lymph nodes smaller than 0.5 cm could be detected by Al^{18}F-HER2-BCH, which were easily missed in either ^{18}F-FDG or other conventional imaging.

Recent advances in breast cancer treatment have showed that, 20-30% developed metastatic disease after the initial diagnosis and treatment of early-stage breast cancer among female breast cancer patients[27]. The four most common metastatic organs associated with breast cancer are bone (50-70%)[28], lung (17%)[27], liver (12-20%) and brain (5-20%)[9]. The patients with metastatic breast cancer had a poor prognosis[29], with a 5-year survival rate of 26%[30], and a reported median survival of 18 to 24 months. In addition, breast cancer patients with liver metastasis have the worst result, with reduced median survival ranging from 14 to 16 months[31 32]. Metastatic diffusion is sometimes difficult to identify on conventional imaging. When patients are first diagnosed clinically after show with symptoms, such as bone pain or hepatitis, the optimal intervention time has been missing[32]. The results showed Al^{18}F-HER2-BCH had a good detection effect for bone and liver metastatic lesions, which could facilitate early clinical intervention. Compared with ^{18}F-FDG and conventional imaging, Al^{18}F-HER2-BCH is a good supplementary means for the detection of liver metastases. Furthermore, Al^{18}F-HER2-BCH showed a lower background in brain than ^{18}F-FDG, which is more conducive to the observation of brain and skull metastases.

The limitation of the present study is the small number of breast cancer patients with limited diversity in HER2 status. In addition, histopathological confirmation of every detected lesion was not feasible due to ethical and practical reasons. Moreover, we did not analyze the relationship between Al^{18}F-HER2-BCH PET imaging and HER2 target treatment in this study. We will further improve the research in a later stage.

Conclusion

Al^{18}F-HER2-BCH PET/CT is feasible for detecting HER2-positive lesions in newly diagnosis and metastatic breast cancer patients and shows better detection ability for small/nonnodule primary lesions, small metastatic lymph nodes, and bone and liver metastases. This approach is helpful for monitoring the expression level of HER2 in lesions and facilitates accurate diagnosis and individualized treatment.

Declarations

ACKNOWLEDGMENTS

The current research was financially supported by Beijing Natural Science Foundation, Jing-Jin-Ji special projects for basic research cooperation (H2018206600), Beijing Excellent Talents Funding (2017000021223ZK33), Beijing Municipal Administration of Hospitals-Yangfan Project (ZYLX201816), Science Foundation of Peking Univesity Cancer Hospital (No.2021-4).

Conflicts of Interest: The authors declare no potential conflicts of interest.

Ethical approval The clinical study was approved by the Medical Ethics Committee of Peking University Cancer Hospital and American Center for Clinical Trial Management (Ethics Approval License

No.2019KT114 and NCT04547309).

Conflicts of interests The authors declare no potential conflict of interests.

Informed consent Informed consent was obtained from the 15 individual participants included in this study.

References

1. Sung H, Ferlay J, Siegel RL, et al. Global cancer statistics 2020: GLOBOCAN estimates of incidence and mortality worldwide for 36 cancers in 185 countries. CA Cancer J Clin. 2021 May;71(3):209–49.
2. Harbeck N, Gnant M. Breast cancer. Lancet. 2017;389(10074):1134–50.
3. Hayes DF. HER2 and Breast Cancer - A Phenomenal Success Story. N Engl J Med. 2019;381(13):1284–86.
4. Mitri Z, Constantine T, O'Regan R. The HER2 Receptor in Breast Cancer: Pathophysiology, Clinical Use, and New Advances in Therapy. Chemother Res Pract. 2012;2012:743193.
5. Maximiano S, Magalhães P, Guerreiro MP, et al. Trastuzumab in the Treatment of Breast Cancer. BioDrugs. 2016;30(2):75–86.
6. Loibl S, Gianni L. HER2-positive breast cancer. Lancet. 2017;389(10087):2415–29.
7. Vernieri C, Milano M, Brambilla M, et al. Resistance mechanisms to anti-HER2 therapies in HER2-positive breast cancer: Current knowledge, new research directions and therapeutic perspectives. Crit Rev Oncol Hematol. 2019;139:53–66.
8. Waks AG, Winer EP. Breast Cancer Treatment: A Review. JAMA. 2019;321(3):288–300.
9. Achrol AS, Rennert RC, Anders C, et al. Brain metastases. Nat Rev Dis Primers. 2019;5(1):5.
10. Goetz MP, Gradishar WJ, Anderson BO, et al. NCCN Guidelines Insights: Breast Cancer, Version 3.2018. J Natl Compr Canc Netw. 2019;17(2):118–26.
11. Bourgeois AC, Warren LA, Chang TT, et al. Role of positron emission tomography/computed tomography in breast cancer. Radiol Clin North Am. 2013;51(5):781–98.
12. Manohar K, Mittal BR, Senthil R, et al. Clinical utility of F-18 FDG PET/CT in recurrent breast carcinoma. Nucl Med Commun. 2012;33(6):591–6.
13. Wahl RL, Siegel BA, Coleman RE, et al. Prospective multicenter study of axillary nodal staging by positron emission tomography in breast cancer: a report of the staging breast cancer with PET Study Group. J Clin Oncol. 2004;22(2):277–85.
14. Fuster D, Duch J, Paredes P, et al. Preoperative staging of large primary breast cancer with [18F]fluorodeoxyglucose positron emission tomography/computed tomography compared with conventional imaging procedures. J Cancer Res Ther. 2008;26(29):4746–51.
15. Lebron L, Greenspan D, Pandit-Taskar N. PET Imaging of Breast Cancer: Role in Patient Management. PET clinics. 2015;10(2):159–95.

16. Avril S, Muzic RF Jr, Plecha D, et al. ¹â,F-FDG PET/CT for Monitoring of Treatment Response in Breast Cancer. J Nucl Med. 2016;57(Suppl 1(Suppl 1):34s-9s.
17. Pritchard KI, Julian JA, Holloway CM, et al. Prospective study of 2-[¹â,F]fluorodeoxyglucose positron emission tomography in the assessment of regional nodal spread of disease in patients with breast cancer: an Ontario clinical oncology group study. J Clin Oncol. 2012;30(12):1274–9.
18. Liu T, Liu C, Xu X, et al. Preclinical Evaluation and Pilot Clinical Study of Al(18)F-PSMA-BCH for Prostate Cancer PET Imaging. J Nucl Med. 2019;60(9):1284–92.
19. Sörensen J, Velikyan I, Sandberg D, et al. Measuring HER2-Receptor Expression In Metastatic Breast Cancer Using [68Ga]ABY-025 Affibody PET/CT. Theranostics. 2016;6(2):262–71.
20. Dijkers EC, Oude Munnink TH, Kosterink JG, et al. Biodistribution of 89Zr-trastuzumab and PET imaging of HER2-positive lesions in patients with metastatic breast cancer. Clin Pharmacol Ther. 2010;87(5):586–92.
21. Tamura K, Kurihara H, Yonemori K, et al. 64Cu-DOTA-trastuzumab PET imaging in patients with HER2-positive breast cancer. J Nucl Med. 2013;54(11):1869–75.
22. Kumar P, Goud SN. Fluorine-18: A radionuclide with diverse range of radiochemistry and synthesis strategies for target based PET diagnosis. Eur J Med Chem. 2020;187:11979.
23. Zhou N, Liu C, Guo X, et al. Impact of (68)Ga-NOTA-MAL-MZHER2 PET imaging in advanced gastric cancer patients and therapeutic response monitoring. Eur J Nucl Med Mol Imaging. 2021;48(1):161–75.
24. Guo X, Zhu H, Zhou N, et al. Noninvasive Detection of HER2 Expression in Gastric Cancer by (64)Cu-NOTA-Trastuzumab in PDX Mouse Model and in Patients. Mol Pharm. 2018;15(11):5174–82.
25. Guo X, Zhou N, Chen Z, et al. Construction of (124)I-trastuzumab for noninvasive PET imaging of HER2 expression: from patient-derived xenograft models to gastric cancer patients. Gastric cancer. 2020;23(4):614–26.
26. Zhou N, Guo X, Yang M, et al. 68Ga-ZHER2 PET/CT Reveals HER2-Positive Metastatic Gastric Cancer With Better Image Quality Than 18F-FDG. Clin Nucl Med. 2020;45(2):e101-e02.
27. Urooj T, Wasim B, Mushtaq S, et al. Cancer Cell-derived Secretory Factors in Breast Cancer-associated Lung Metastasis: Their Mechanism and Future Prospects. Curr Cancer Drug Targets. 2020;20(3):168–86.
28. Tahara RK, Brewer TM, Theriault RL, et al. Bone Metastasis of Breast Cancer. Adv Exp Med Biol. 2019;1152:105–29.
29. Barco I, Garcia-Font M, García-Fernández A, et al. Breast cancer patients developing distant metastasis at follow-up: Mortality-related factors. Breast J. 2021;27(3):291–93.
30. Peart O. Metastatic Breast Cancer. Radiol Technol. 2017;88(5):519M-39M.
31. Rahnemai-Azar AA, Selby LV, Lustberg MB, et al. Surgical Management of Breast Cancer Liver Metastasis. Surg Oncol Clin N Am. 2021;30(1):27–37.

32. Diamond JR, Finlayson CA, Borges VF. Hepatic complications of breast cancer. *Lancet Oncol*. 2009;10(6):615–21.

Tables

Due to technical limitations, table 1 to 3 is only available as a download in the Supplemental Files section.

Figures

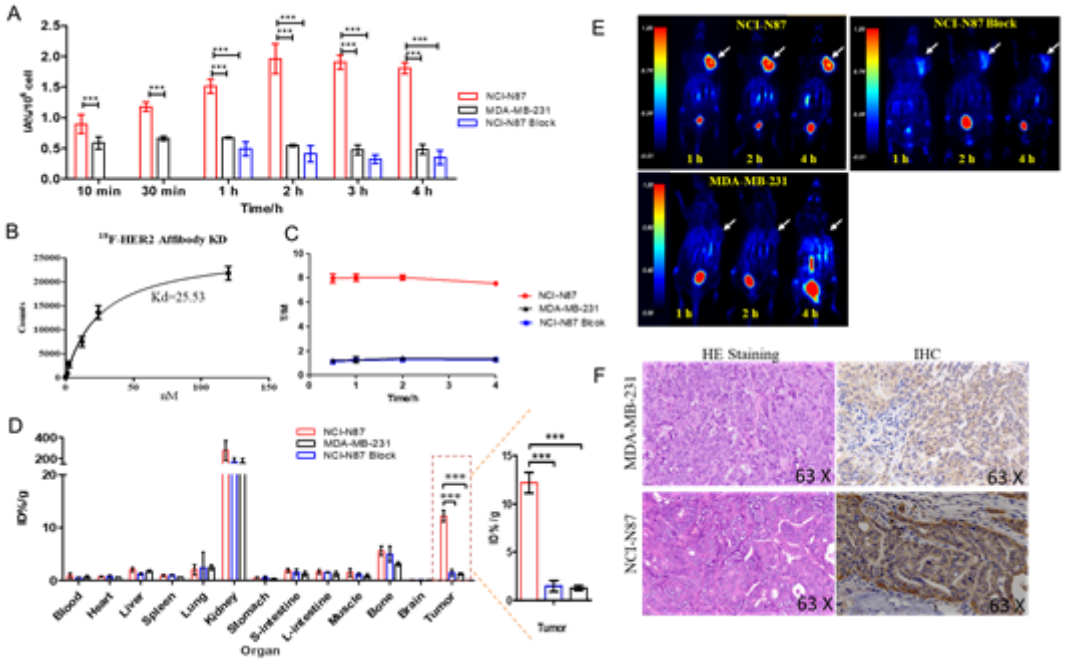

Figure 1

Preclinical study of Al18F-HER2-BCH. (A) Cell uptake study of Al18F-HER2-BCH in three groups as NCI-N87 cells, MDA-MB-231 cells , and NCI-N87 cells with block; (B) Kd study of Al18F-HER2-BCH in NCI-N87 cell line; (C) Broken line diagram of tumor to muscle (T/M) ratio versus time in the whole imaging process of three groups as NCI-N87 models, MDA-MB-231 models , and NCI-N87 models with block; (D) Bio-distribution study of Al18F-HER2-BCH in NCI-N87 group, MDA-MB-231 group, and block group; (E) Micro-PET study in NCI-N87 group, MDA-MB-231 group, and block group; (F) the results of HE staining and IHC of NCI-N87 tumors and MDA-MB-231 tumors.

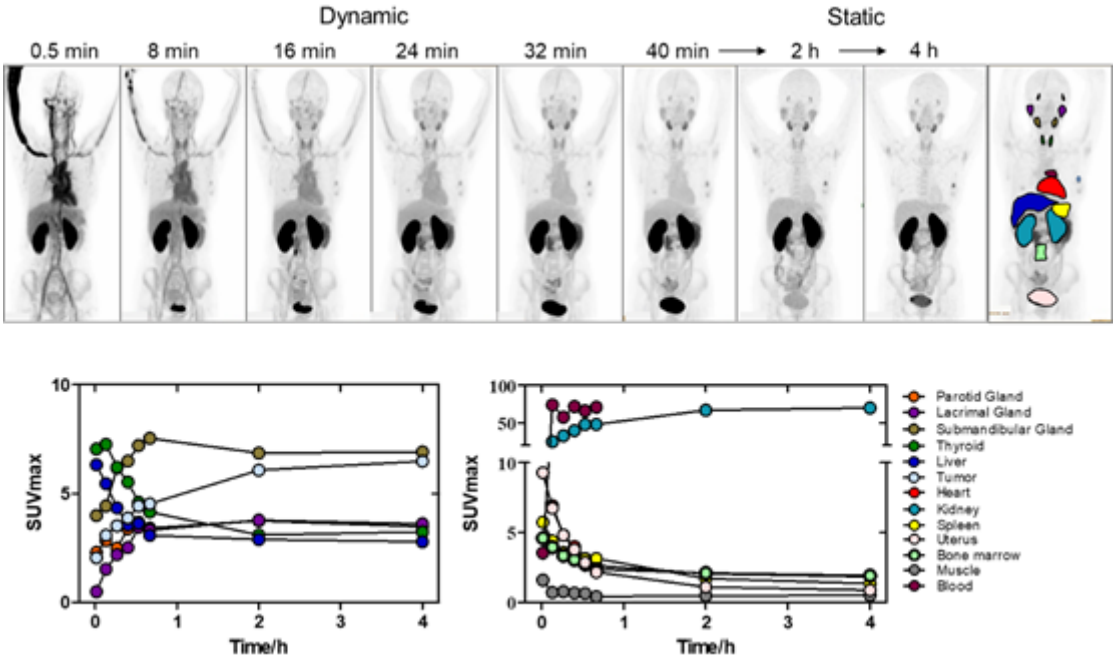

Figure 2

Dynamic imaging study of Al18F-HER2-BCH during 0.5min-40min, static imaging study at 2h and 4 h, and distribution curve of normal tissues.

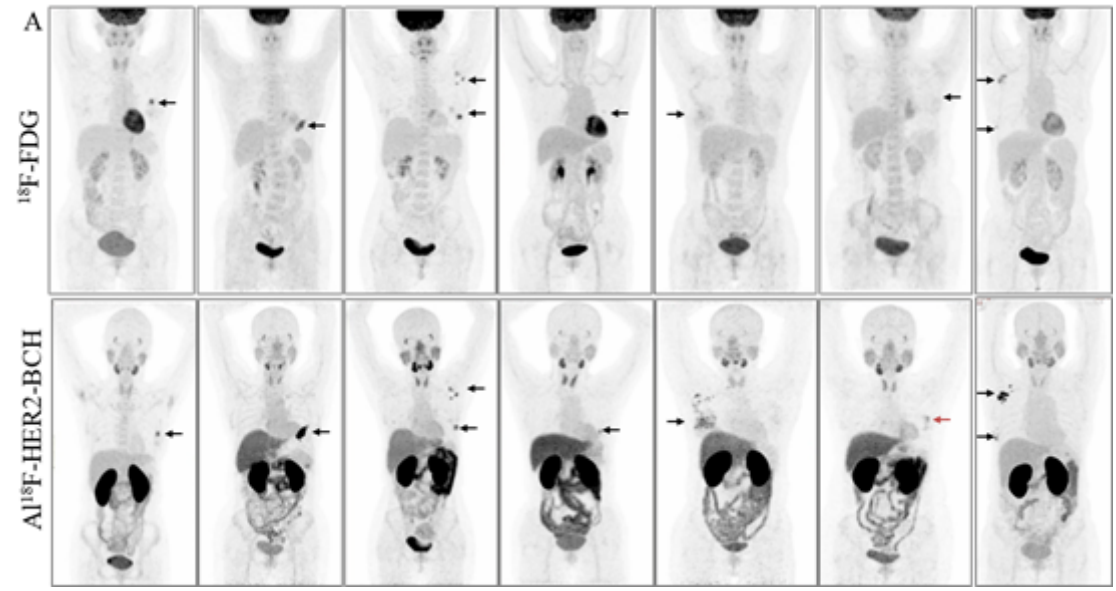

Figure 3

The anterior maximum intensity projection image obtained at 18F-FDG and Al18F-HER2-BCH PET in 7 primary breast cancer patients.

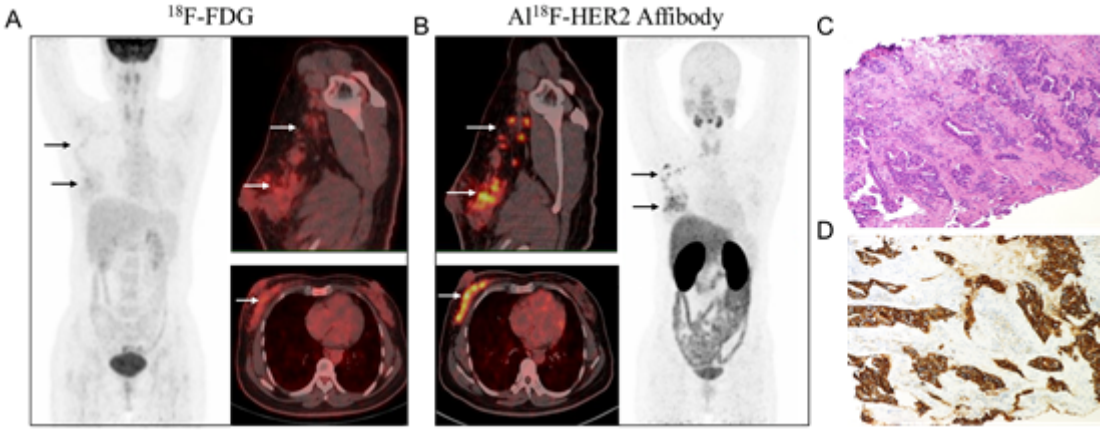

Figure 4

(A) Images of 18F-FDG PET/CT in a HER2-positive primary diffuse breast cancer patient. (B) Images of 18F-FDG PET/CT in the same patient; The HE staining (C) and IHC (D) test of the patient.

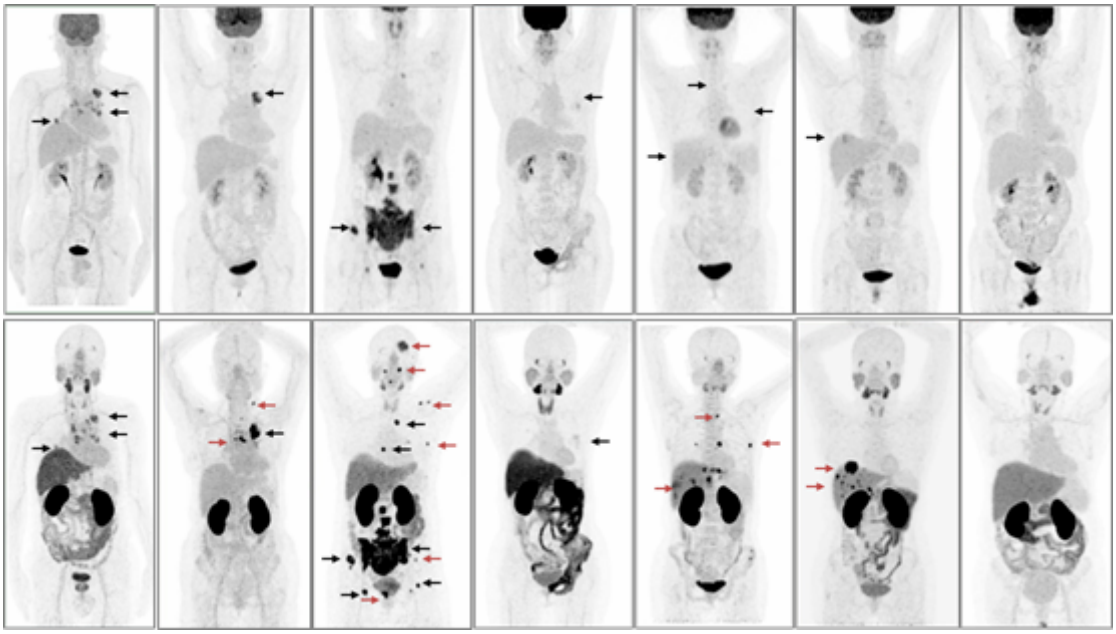

Figure 5

Images of 18F-FDG PET and Al18F-HER2-BCH in 7 relapse and metastatic breast cancer patients. The black arrow showed the lesions detected by both 18F-FDG and Al18F-HER2-BCH, and the red arrow showed the lesions detected only by Al18F-HER2-BCH.

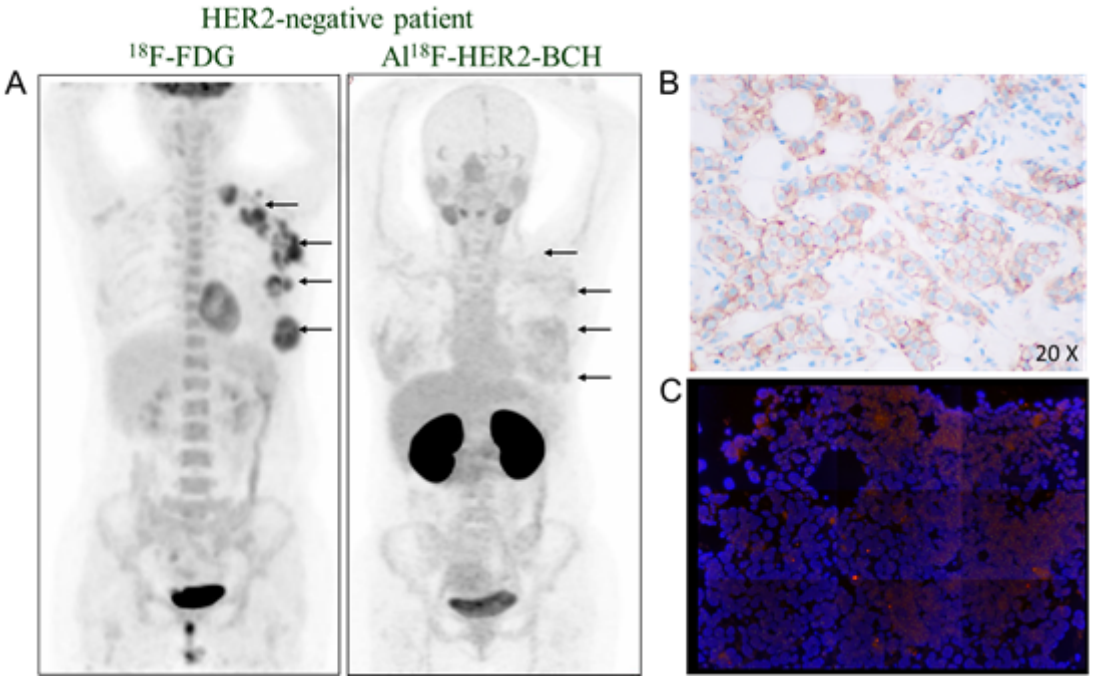

Figure 6

(A) Images of 18F-FDG PET/CT in a HER2-negative metastatic breast cancer patient. (B) Images of 18F-FDG PET/CT in the same patient; The HE staining (C) and IHC (D) test of the patient.

Supplementary Files

This is a list of supplementary files associated with this preprint. Click to download.

- Tables.docx
- SupplementInformation.docx